Multistability and transitions between spatiotemporal patterns through versatile Notch-Hes signaling

Benjamin Pfeuty

Multistability and transitions between spatiotemporal patterns through versatile Notch-Hes signaling

Benjamin Pfeuty

Univ. Lille, CNRS, UMR 8523 – PhLAM – Physique des Lasers Atomes et Molécules, F-59000 Lille, France

Email address: benjamin.pfeuty@univ-lille.fr (Benjamin Pfeuty)

Multistability and transitions between spatiotemporal patterns through versatile Notch-Hes signaling

Benjamin Pfeuty

Univ. Lille, CNRS, UMR 8523 – PhLAM – Physique des Lasers Atomes et Molécules, F-59000 Lille, France

Abstract

The Delta-Notch-Hes signaling pathway is involved in various developmental processes ranging from the formation of somites to the dynamic fine-grained patterns of cell types in developing or regenerating tissues. Such broad patterning capabilities rely in part in the versatile and tunable dynamics of the Notch-Hes feedback circuit eliciting both pulsatile and switching behaviors. This raises the theoretical issue of which specific spatiotemporal features emerges from lateral inhibition between cells that can display and transit between steady, oscillatory and bistable regimes. To address this issue, we consider a discrete cell lattice model where intracellular dynamics is described by a phase-like variable and displays a typical cross-shaped phase diagram. Model analysis identifies how the existence and stability of many spatially-inhomogeneous and temporally-synchronized patterns depends on key intracellular and intercellular parameters, which highlights an extensive multistability between those diverse spatiotemporal patterns as well as the existence of multiple robust transition scenarios from temporal patterns to spatial patterns. Such broad repertoire and multistability of spatiotemporal patterns is corroborated using a signaling network model of the Notch-Hes pathway.

Keywords:
Multicellular development, Pattern formation, Oscillations, Cell-fate decision, Multistability

Email address: benjamin.pfeuty@univ-lille.fr (Benjamin Pfeuty)

Introduction

The interplay between Notch-mediated intercellular communications and Notch-driven intracellular activities is an important source of self-organized developmental patterns across metazoan tissues (Andersson et al., 2011; Siebel and Lendahl, 2017; Henrique and Schweisguth, 2019; Boareto, 2020). The interaction between Delta ligands and Notch receptors depends on many cell-specific features including the types and the spatial distribution of ligands and receptors (Sprinzak et al., 2010; Shaya et al., 2017; Nandagopal et al., 2018). In turn, Notch is prone to inhibit the production of Delta ligands through diverse indirect and direct signaling mechanisms involving the Hes family of proteins (Kageyama et al., 2007; Sjöqvist and Andersson, 2019). Hes proteins does not only mediate Notch-dependent repression of Delta or fate-inducing proteins, but its autorepression is a source of intracellular oscillations that is prone to occur prior fate commitment in developing and regenerating tissues (Kageyama et al., 2007, 2018). Notch-Hes pathway also contributes to cell-fate decision programs by antagonizing some fate-promoting factors and reciprocally (Roese-Koerner et al., 2016; Wahi et al., 2016; Sagner et al., 2018). This specific ability of Notch signaling pathway to elicit both oscillatory and switching activities is prone to give rise to diverse and complex spatiotemporal patterns of cell fates within tissues (Biga et al., 2021; Uriu et al., 2021), whose repertorie has yet to be fully explored and characterized.

From a modeling viewpoint, a primary patterning role of Delta-Notch intercellular coupling is to destabilize homogeneous states and promote fine-grained patterning through a spatial symmetry-breaking process triggered by the mutual inhibition between nearest-neighboring cells (Collier et al., 1996). This seminal model has been further refined to illustrate how positive feedback, protrusions, signaling crosstalks or cell division can modulate the relative stability or occurence of diverse -periodic or aperiodic- spatial patterns (Wearing et al., 2000; Hunter et al., 2016; Hadjivasiliou et al., 2016). In developmental contexts where Notch-Hes signals contribute to cellular oscillations, various models, using a discrete or continuous description of tissues and using a phase-like or biochemical description of oscillators, have been used to capture the emergence of patterns such as traveling waves (Murray et al., 2011, 2013; Jörg et al., 2015; Tomka et al., 2018), antiphase synchrony (Lewis, 2003; Wang et al., 2011) or dynamic clusters (Biga et al., 2021). However, a consistent theoretical framework is still lacking to study the coexistence and transition between synchronized patterns of oscillatory cells and spatial patterns of bistable cells in various developmentals contexts. This issue of dynamical routes toward tissue patterning has been nevertheless investigated for some specific developmental contexts and modeling settings (Owen, 2002; Plahte and Øyehaug, 2007; Fujimoto et al., 2008; Koseska et al., 2010; Suzuki et al., 2011; Murray et al., 2011; Pfeuty and Kaneko, 2014; Stanoev et al., 2021), including cell type-specific regulatory network models (Pfeuty, 2015; Keskin et al., 2018; Tiedemann et al., 2017).

In this study, we develop a modeling framework that combines minimal modeling and signaling network modeling in order to study developmental transitions between temporal to spatial patterns as those

driven by Notch-Hes pathway. First, we introduce an effective model of Notch-Hes intracellular dynamics whose low-dimensional parameter and state spaces eases theoretical analysis of spatiotemporal dynamics of cell population. Under some assumption about intercellular coupling and lattice topology, the stability analysis of several archetypical classes of spatiotemporal patterns reveals the existence of signal-dependent multistability between synchronization and inhomogeneous stationary states states. Biological implications of multistable patterns are investigated at the level of developmental transition scenarios from temporal to spatial patterns or by assessing the validity of the theoretical results in simulations of more realistic systems biology models.

Results

A minimal model of oscillatory-bistable cells coupled through lateral inhibition

Previous models of the intracellular Notch-Hes pathway frequently display both oscillatory and bistable behaviors depending on some key parameters (Agrawal et al., 2009; Goodfellow et al., 2014; Pfeuty, 2015), typically organized as a typical cross-shaped phase diagram where the transition between oscillation to bistability can occur through diverse codimension-2 bifurcation (Boissonade and De Kepper, 1980; Pfeuty and Kaneko, 2009). To further simplify the description of single-cell dynamics featured with oscillation and bistability, we propose an effective one-dimensional model adapted from the so-called *theta* model whose dynamics is described by a single angular variable. Initially introduced as the canonical model for a neuron which undergoes a saddle-node on invariant circle (SNIC) bifurcation as external current increases (Ermentrout, 1996; Laing, 2016), the model can be slightly modified to describe a transition from oscillation to bistability through a two-SNIC bifurcation:

$$\frac{d\theta}{dt} = 1 - \cos(2\theta) - S_D\,(1 + \cos(2\theta)) + S_N \cos(\theta) \equiv f(\theta, S_D, S_N) \tag{1}$$

The phase diagram exhibits monostable, bistable and oscillatory domains which are symmetrically organized as function of S_D and S_N (Fig. 1A). The existence of and transition between these dynamical states are easily explained by the manner how the 2π periodic velocity field changes with S_D and S_N (Fig. 1(B)). Of note, the reduced form $\frac{d\theta}{dt} = 1 - \cos(2\theta)$ for $S_D = S_N = 0$ corresponds to the codimension-2 two-SNIC bifurcation for the transition between oscillations and bistability.

In the context of Notch-driven developmental patterning, the phase of the angular variable represents high/low value of Notch and Hes for $\theta \sim \pi/0$. While S_N represents Notch signaling cues, S_D represents other signaling cues (such as FGF or retinoic acid) or epigenetic cues (such as Id), which are known to interfere with intracellular oscillations and eventually promote stable cell-fate choice. The manner how S_N of the receiver cell i depends on the state θ of the sender cells j must be also 2π-periodic and is chosen as following:

$$S_N = S_{N0} + \gamma \cos(\theta_j(t - \tau_j)), \tag{2}$$

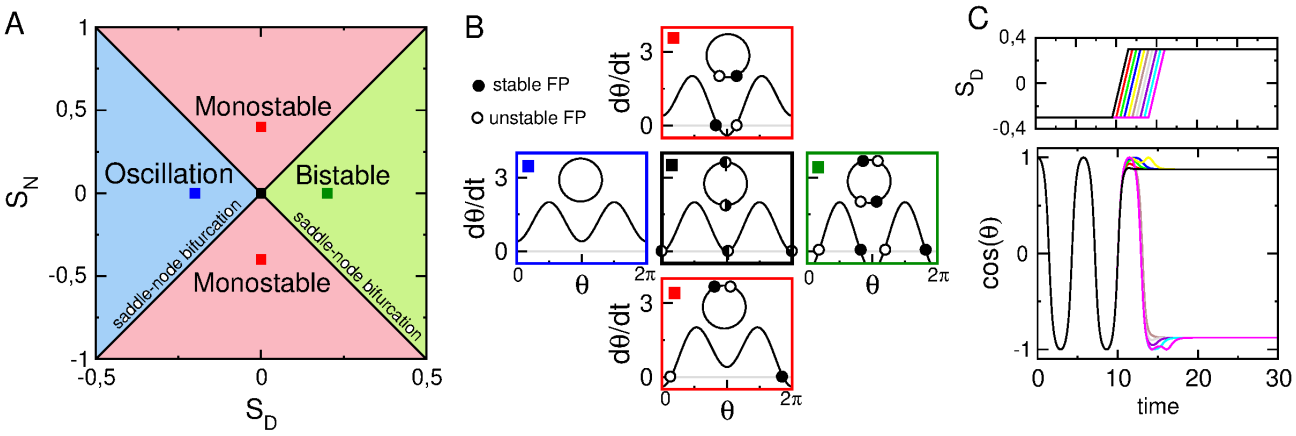

Figure 1: **A low-dimensional model of oscillatory/bistable single-cell dynamics** (A) Phase diagram in the signal parameter space S_D and S_N. (B) Vector fields associated with the regime of oscillations (left), bistability (right), monostability (up and down) and the co-dimension 2 saddle-node bifurcation (center). (C) Signal-driven transition from a single-cell oscillations to distinct steady states depending on signal timing

to implement the lateral inhibition property: the coupling term $\gamma \cos(\theta_i)\cos(\theta_j)$ becomes negative and stabilizing for different cell states ($\theta_j = \theta_i + \pi$), and positive and destabilizing for same cell states ($\theta_j = \theta_i$). The delay τ represents the signaling delays associated to this lateral inhbition.

The population system can thus be written without loss of generality as

$$\frac{d\theta_i}{dt} = f(\theta_i, S_D, S_{N0}) + \Gamma/N \cos(\theta_i) \sum_{j=1,N} J_{ij} \cos\left(\theta_j(t-\tau)\right). \tag{3}$$

To account for the juxtacrine communication of Delta-Notch, we consider a coupling matrix $J_{ij} = 1$ for the nearest-neighbor cells and zero otherwise. The global coupling strength $\Gamma = N\gamma$ with a number of neighboring cells of $N = 2$ for 1D array, $N = 8$ for a square lattice or $N = 6$ for an hexagonal lattice.

Multistability between synchronization states and inhomogeneous steady states

A comprehensive analysis of the spatiotemporal patterning in the cell population model (Eq. (3)) is made possible by the relatively low number of control parameters (Fig. 2(A)). The property of intercellular coupling is monitored at the level of the coupling strength Γ and delay τ. In addition, the symmetric phase diagram as function of the two parameters S_D and S_N (Fig. 1(A)) provides also the possibility to study how spatiotemporal patterning depends on qualitative change in single-cell dynamics through continuous parameter changes. To further simplify the analysis, we consider a ring lattice topology with homogeneous signaling ($S_{D,i} = S_D$ and $S_{N0,i} = S_{N0} = 0$), which left us with S_D, Γ and τ as the main control parameters (Fig. 2(A,B)).

A basic class of non-stationary pattern are phase-locked synchronization states (PSS) where neighboring oscillatory cells displays a constant phase shift ψ or time shift $\Delta = \psi\frac{T}{2\pi}$. $\Delta = 0$ and $T/2$ correspond to in-phase and anti-phase synchronized states while other values can be seen as uniform traveling (or rotating) waves. With a one-dimensional ring topology, the phase-locked condition reads $\theta_{i+1}(t) = \theta_i(t + \Delta)$ which

can be replaced in Eq. (3) to obtain:

$$\frac{d\theta_i}{dt} = f(\theta, S_D, 0) + \Gamma \cos(\theta_i) \left[\cos(\theta_i(t-\tau-\Delta)) + \cos(\theta_i(t-\tau+\Delta)\right]/2\,. \tag{4}$$

Defining the T-periodic delay function $H_u(\theta(t)) = \theta(t) - \theta(t-u)$ (that satisfies $H_0 = 0$ or $H_{u+v} = H_u + H_v$), trigonometric relations can then be used to obtain:

$$\frac{d\theta_i}{dt} = f(\theta_i, S_D, 0) + \Gamma \cos(\theta_i) \cos(H_\tau(\theta_i))(\cos(\theta_i)\cos(H_\Delta) + \sin(\theta_i)\sin(H_\Delta))\,. \tag{5}$$

In the particular cases of in-phase synchronized solution with no coupling delay ($\Delta = \tau = 0$) and anti-phase synchronized solution with half-period delay ($\tau_\Delta = \tau = T/2$), Eq.(5) reduces to $\dot{\theta} = f(\theta, S_D - \Gamma/2, 0)$ for which a periodic solution exists only for $S_D < \Gamma/2$ (Fig. 1(A)) defining a maximal bound for the existence of PSS (Fig. 2(B)).

Stability analysis of phase-locked solutions $\theta_{i+1}(t) = \theta_i(t+\Delta)$ of identical oscillators could be done by linearizing around the periodic solution manifold and compute Floquet multipliers or exponents. We use a more heuristic approach that is to simulate the response of the full system to small spatially-periodic transverse perturbation $\delta\theta$ ($\delta\theta_i(0) = -\delta\theta_{i+1}(0) = \delta\theta_{i+2}(0)$) and evaluate whether such perturbation is relaxed or amplified after one period. Phase diagram shows that relative stability of different phase-locked solutions (e.g., $\Delta = 0$, $T/2$ and $T/25$) essentially depends on coupling delays such that phase multistability can naturally occur for some values of coupling strength and delays (Fig. 2(B)). Besides synchronization states, incoherent state attractors are also observed (lower left panel of Fig. 2(C)) but are beyond the scope of this study.

This system also displays stationary spatial patterns such as spatially periodic patterns in which cells settle in two states $\theta_{i=1,2}$ with a fixed proportion $k_{i=1,2}$ (i.e., order parameters) of neighbors in different states. In case of a square lattice, $k_{1,2} = 0.75$ for a 1-cell stripe pattern, $k_{1,2} = 0.5$ for a 1-cell or 2-cell checkerboard pattern, $k_{1,2} = \{0.125, 1\}$ for the spot/gap pattern and $k_{1,2} = \{0.375, 0.75\}$ for the 2-cell/1-cell stripe pattern. In case of a hexagonal lattice, $k_{1,2} = 2/3$ for a 1-cell stripe pattern and $k_{1,2} = \{1/3, 1\}$ for the spot/gap pattern. For a one-dimensional lattice, $k_{1,2} = 1$ for the 1-cell stripe pattern. For any of these patterns, steady-state solultion of Eq. (3) can be casted into two equations associated to $d\theta_{1/2}/dt = 0$ as,

$$F(\theta_{1/2}, S_D, S_{N0}) + \Gamma \cos(\theta_{1/2}) \left((1-k_{1/2})\cos(\theta_{1/2}) + k_{1/2}\cos(\theta_{2/1})\right) = 0\,. \tag{6}$$

A particular steady-state solution corresponds to a saddle-node instability for each cell type, which coincides with the appearance or disappearance of an inhomogeneous stationary state. Such instability necessarily occurs for $\theta_1 = 0$ and $\theta_2 = \pi$ which are replaced in Eq. (6) to finally obtain a set of relation between $k_{1/2}$,

Γ and $S_{D/N0}$ as:

$$-2(S_D - \Gamma(1-k_1)/2) - \Gamma k_1 + S_{N0} = 0 \tag{7a}$$

$$-2(S_D - \Gamma(1-k_2)/2) - \Gamma k_2 - S_{N0} = 0 \tag{7b}$$

Summing these equations cancels out S_{N0} to finally derive the critical coupling strength for which the inhomogeneous state is destabilized:

$$\Gamma = \frac{2S_D}{1-k_1-k_2} \equiv \Gamma_c \tag{8a}$$

$$S_D = \frac{\Gamma}{2}(1-k_1-k_2)/2\,. \tag{8b}$$

The above condition for saddle-node instability boundary thus delimits the stability domain of an inhomogeneous steady state (ISS) defined by the order parameter $k_1 + k_2$. On the one hand, spatial patterns for which neighboring cells are in average more similar than different ($k_1 + k_2 < 1$) are destabilized above some inhibitory coupling strength $\Gamma > \Gamma_c > 0$ when cells are bistable $S_D > 0$, such as the fully homogeneous state ($k_{1/2} = 0$) destabilized for $\Gamma > 2S_D$ (Fig. 2(B)). On the other hand, spatial patterns for which neighboring cells are in average more different than similar (i.e., $k_1 + k_2 > 1$) are always stable for $S_D > 0$ ($\Gamma_c < 0$) and are stabilized above some inhibitory coupling strength $\Gamma > \Gamma_c = \frac{2S_D}{1-k_1-k_2}$ for oscillatory cells ($S_D < 0$), supporting a scenario of oscillation amplitude death. Numerical simulations show that lateral inhibition can stabilize non-periodic spatial patterns for which neighboring cells are more different than similar, such as labyrthin pattern for which $k_i = 5/8$ or $6/8$ (lower right panel of Fig. 2(C)).

These stability properties of phase-locked synchronized states (PSS) and inhomogeneous steady states (ISS) reveal two key complementary features of the spatiotemporal dynamics of oscillatory/bistable cells coupled through delayed inhibition between nearest neighbors. Lateral inhibitory coupling stabilizes ISS even when uncoupled cells oscillate and PSS even when uncoupled cells are in steady states. As a result, the multicellular system exhibits a robust multistability between PSS and ISS especially when uncoupled cells are operating close enough to the transition between oscillation and bistability (i.e., $|S_D| < \Gamma$). Accordingly, multiple stationary or non-stationary attractors can coexist such as those satisfying spatial periodicity $\theta_{i+2}(t) = \theta_i(t)$ (Fig. 2(D)), such that attractor selection would depend on the initial conditions. It is important to note that this extensive multistability property does not occur for negative value of Γ and is therefore mediated by the lateral inhibitory coupling.

Pattern selection through transition from temporal to spatial patterns

The class of biological phenomena that motivates the present theoretical study concerns the developmental transition whereby a given population of oscillatory cells gives rise to two subpopulations of well-distinct cell states. In particular, a pending question is the ability of Notch pathways to underlie very diverse

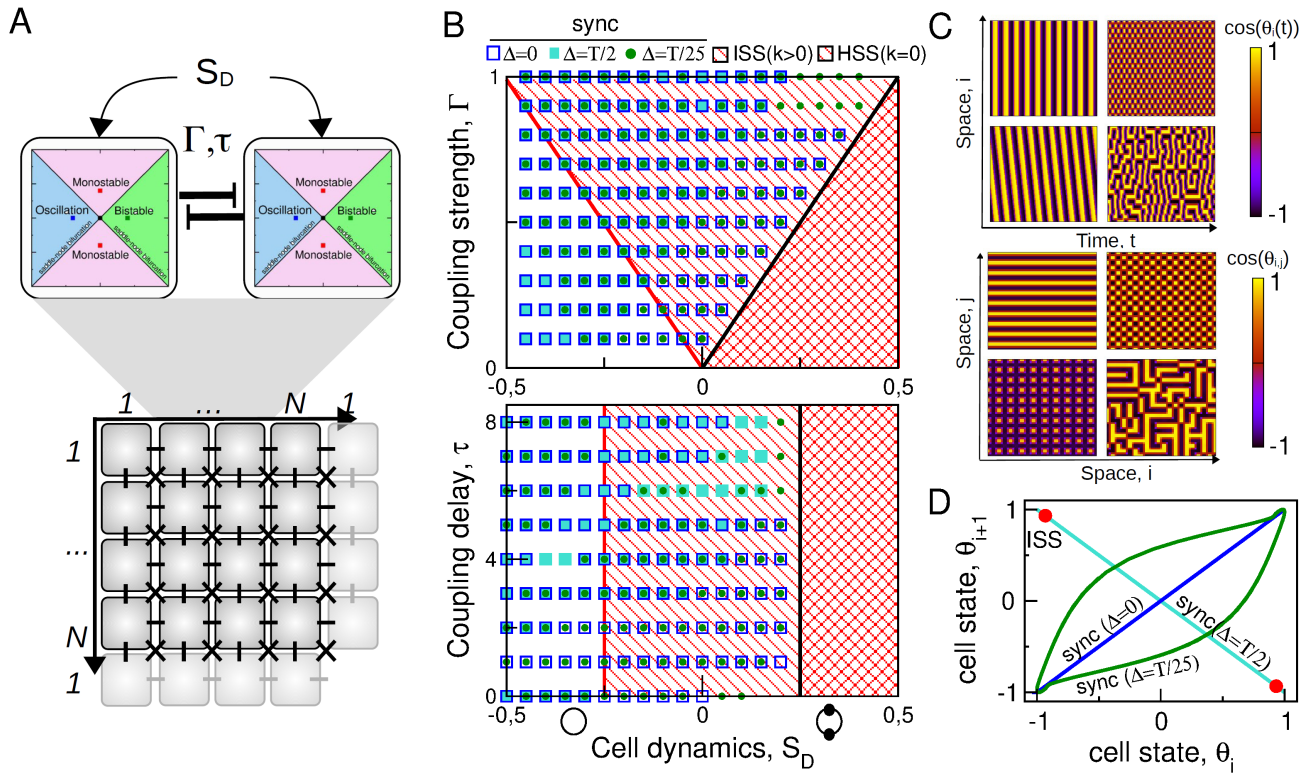

Figure 2: **Spatiotemporal dynamics of inhibitory-coupled oscillatory/bistable cells.** (A) Cell population model organized as a 1D or 2D periodic lattice with first-neigbor inhibitory coupling. (B) Stability domains of typical phase-locked synchronization states and spatial stationary states as function of S_D and Γ (top: $\tau = 3$), and as function of S_D and τ (bottom: $\Gamma = 0.5$). (C) Example of stable temporal patterns for a 1D lattice with $\Gamma = 0.5$, $\tau = 3$ and $S_D = 0$ (up panels) and of stable spatial patterns for a 2D lattice with $\Gamma = 0.5$ and $S_D = 0$ (Down panels). (D) Example of multistability between phase-locked synchronization states (PSS) and inhomogeneous spatial states (ISS) in the 1D lattice plotted in the phase plane $\{\theta_i, \theta_i + 1\}$ for $S_D = -0.1$, $\Gamma = 0.5$ and $\tau = 3$.

symmetry-breaking scenarios from temporal to spatial patterns, involving stripe patterns as during somitogenesis or salt-and-pepper patterns as during neurogenesis. This issue is addressed in the population model (Eq. (3)) by simulating the spatiotemporal dynamics in response to a temporal increase S_D corresponding to a slow developmental change of signaling or epigenetic cues. According to the repertoire and stability domains of states identified in Fig. 2, the population can be prepared and settled for $S_D(t = 0) = S_{D1} < 0$ into diverse spatiotemporal states such as in-phase synchronization, traveling waves and antiphase synchronization (Fig. 3). By stabilizing these states, intercellular coupling provides robustness to diverse sources of noise, here in the initial conditions and in the signal dynamics $S_D(t)$. Following an increase of S_D, each temporal pattern gives rise to a specific stationary pattern depending on the spatial pattern at the time of the differentiation signal increase and the profile of such increase. First, a synchronous oscillatory pattern translates into a homogeneous stationary pattern as far as $S_{D2} > \Gamma/2$ (Fig. 3(A)). Second, a traveling wave pattern translates into a regular stripes (Fig. 3(B)) produces stripes of tunable size as far as $S_D(t = t_f)$ is sufficiently high to stabilize these stripe patterns. Last, an antisynchronous pattern translates into an inhomogeneous stationnary pattern stripe pattern of one-cell width in 1D (Fig. 3(C)). In these transition processes, the role of lateral inhibition in stabilizing phase shifts between neighboring cells is very effec-

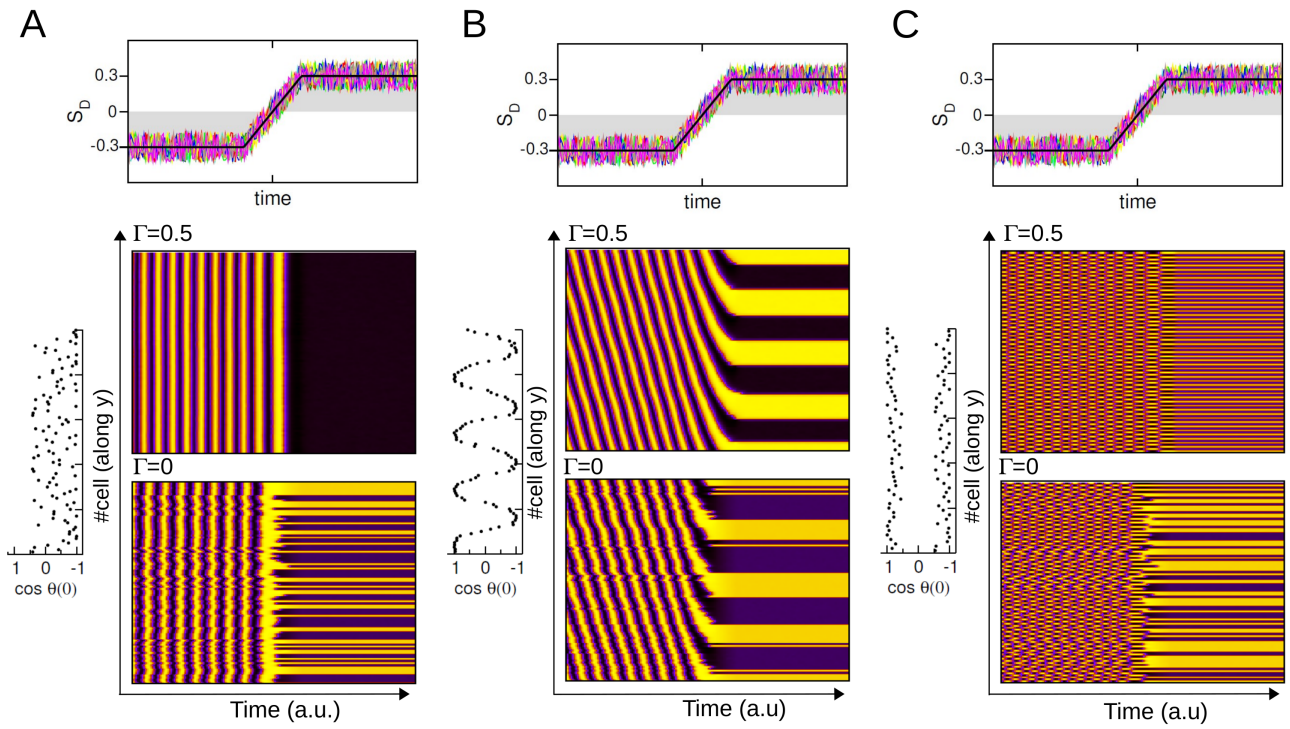

Figure 3: **Robust and tunable transition routes from temporal to spatial patterns.** Transient spatiotemporal dynamics from a noisy initial spatial pattern $\theta_i(0)$ for $S_D(t) < 0$ (left panels of A-C) and driven by a noisy temporal pattern $S_D(t) = S_{D1} + (S_{D2} - S_{D1})\mathcal{H}(t) + \zeta(t)$ where $S_{D1} = -0.3$ and $s_{D2} = 0.2$ (uppest panel of A-C). The spatiotemporal dynamics $\cos(\theta_i(t))$ is compared with and without coupling ($\Gamma = 0.5$ for the upper-right panel and $\Gamma = 0$. for the lower-right panel). (A) From a noisy initial conditions, lateral inhibition promotes a robust transition from synchronous oscillations to an homogeneous spatial pattern. (B) From a noisey and spatially-periodic initial conditions, lateral inhibition promotes a robust transition from a traveling wave pattern to a regular stripe pattern. (C) From noisy checkerboard noisy intial conditions, lateral inhibition promotes a robust transition from antisynchronous oscillations to a checkerboard spatial patterns.

tive to obtain regular and defect-free spatial patterns (compare dynamics with and without coupling in Fig. 3(A,B,C)).

Multistable spatiotemporal patterns in a systems biology model of Delta-Notch-Hes circuit

To assess the biological relevance of results obtained with effective low-dimensional intracellular dynamics, we develop a systems biology model of Delta-Notch-Hes pathways whose feedback architecture enables a cross-shaped diagram similar to Fig.1(A). Previous single-cell models have first focused on the core autorepression of Hes1 protein (Lewis, 2003) before to incorporate additional set of factors mutually interacting with Notch or Hes, such as Rbpj (Agrawal et al., 2009), miR9 (Goodfellow et al., 2014), Cyclins-Cdks (Pfeuty, 2015) or Neurog (Tiedemann et al., 2017). Such interlocking between a core negative feedback mediated by Hes autorepression, and positive feedback mediated by mutual inhbition between Notch or Hes and other cell fate-specific factors is indeed a common feature in various tissues and cell types (Fig. 4(A)). For instance, members of Hes family proteins mutually antagonize with transcription factors including miR9 or Ascl1 in neural progenitors (Roese-Koerner et al., 2016; Vasconcelos et al., 2016), Olig2 in motoneuron progenitors (Sagner et al., 2018), Neurog3 in multipotent pancreatic progenitor cells (Ahnfelt-Rønne et al., 2012), Myod in myoblast (Lahmann et al., 2019) and Lfng or Mesp2 in presomitic stem cells (Wahi et al.,

2016). Alhtough the detailed set of regulatory mechanisms can differ depending on cell type, we can nevertheless develop a generic model where Notch, Hes and Delta concentration variables are supplemented with an antagonistic factor, named Y (Fig. 4(B)), based on the model of Delta-Notch-Hes-miR9 circuit developed in (Pfeuty, 2015):

$$\tau_N \frac{dN}{dt} = \frac{S_N}{1 + \mathbf{S_N} + k_{YN} Y^2} - N \tag{9a}$$

$$\tau_{H_m} \frac{dH_m}{dt} = \frac{k_{NH} N^2}{1 + k_{HH}\,(1 + k_{FH}\,S_{Dif}) H(t - \tau_1)^n + k_{NH} Y^2} - H_m \tag{9b}$$

$$\tau_H \frac{dH}{dt} = H_m(t - \tau_2) - d_H H \tag{9c}$$

$$\tau_Y \frac{dY}{dt} = \frac{1}{1 + k_{FY} S_{Dif}^2 + k_{HY} H^2} - Y \tag{9d}$$

$$\tau_D \frac{dD}{dt} = \frac{1}{1 + k_{HD} H^2} - D \tag{9e}$$

$$S_{N,i} = S_{N0,i} + \gamma \sum_j D_j(t - \tau) \tag{9f}$$

where N represents Notch activity, H_m and H represent concentrations of Hes mRNA and proteins, D represents Delta ligand and Y represents a fate-specific factor antagonizing with Notch and/or Hes proteins. Regarding signaling cues, S_N represents the extracellular juxtacrine signals associated with Delta-dependent activation of Notch receptor while S_{Dif} represents an extracellular morphogenetic fields associated with relative concentrations of extracellular signals (such as FGF and RA) assumed to promote expression of Y and inhibiting autorepression of H.

Degradation and time-delay parameters of the model (τ_i) are set with agreement with experimental measurements and the approximate 2-hour period of Hes oscillation (Pfeuty, 2015). In the case where the species Y is weakly expressed associated to S_{Dif} low (e.g., low RA and high FGF), the Notch-Hes regulatory module displays oscillations for intermediate Notch signal S_N. In the case where the species Y is highly expressed associated to S_{Dif} high (e.g., high RA and low FGF), the concomittant decrease of Hes autorepression leads to a robust bistability due to mutual inhibition between Notch-Hes and Y. Given these two archetypical oscillation and bistable behaviors obtained for low and high S_{Dif} level, the parameters for mutual inhibtion between Hes and Y are then adjusted to obtain a phase diagram similar with the low-dimensional model for the sake of comparison (Fig. 4(C) as compared to Figure 1(A)). Although biochemical and low-dimensional models share a similar cross-shaped phase diagram, it is to mention that the detailed model shows a more complex bifurcation scenario where the transition between oscillation and bistability occurs typically through a concomittant Hopf and saddle-node bifurcation (instead of a two-SNIC bifurcation). These fine-grained dissimilarities do not impact the coarse-grained transition behavior whereby increase of S_{Dif} leads to a cellular transition from an oscillatory state toward diverging steady states depending on the relative timing between signal course and oscillatory phase (Figure 4(D) as compared to

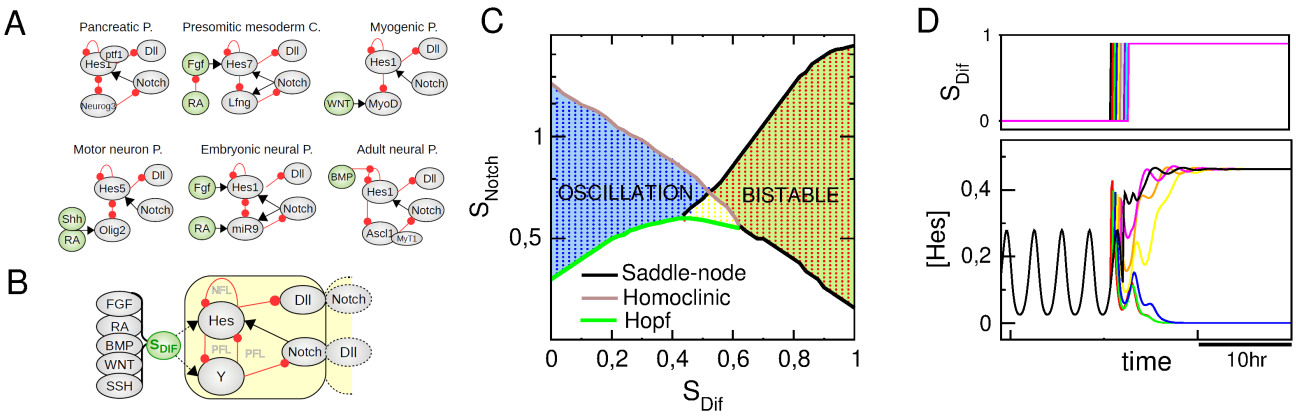

Figure 4: **Oscillation and bistability in a systems-biology model of Notch-Hes signaling.** (A) Feedback regulatory circuits involved in Notch/Hes-driven fate decision in various tissue-specific cell types. (B) Schematic network model of the Notch-Hes-Delta circuit based on the common features of cell type-specific circuits in (A). (C) Phase diagram with a transition from oscillation to bistability obtained for the following parameter set: $d_N = 1$, $d_H = d_Y = 2$, $d_{mH} = 10$, $k_{NH} = 10$, $k_{HY} = 17$, $k_{YH} = 7$, $k_{YN} = 7$, $k_{FY} = 0.25$; $\tau_{1,2} = 0.5$h. (D) Example of a transition from single-cell oscillations to distinc steady statesas function of the timing of S_{Dif} increase.

Figure 1(C)).

To address again the spatiotemporal dynamics of oscillatory/bistable cells coupled through Delta-Notch, we consider a periodic 1D lattice with homogeneous signaling field, in order to define the same setting used for the theoretical analysis of the simple model (Fig.5(A)). Multistability between diverse spatiotemporal patterns are investigated through adiabatic increase of S_{Dif} starting from stable inphase or antiphase synchronization states for small S_{Dif} values and through adiabatic decrease of S_{Dif} starting from a typical inhomogeneous stationary states of 1-cell period (Fig.5(B)) Simulation shows that Delta-Notch intercellular communications can stabilize (i) inhomogeneous steady states (ISS) even for cells oscillating without coupling ($S_{Dif} < 0.5$) and (ii) phase-locked synchronized states (PSS), both synchronous and antisynchronous depending on coupling delay, even for stationary cells without coupling ($S_{Dif} > 0.5$), indicating a robust multistability between PSS and ISS. for intermediate differentiation signals. Such extensive multistability between stationary and nonstationary patterns is exemplified for some intermediate value of coupling delay $\tau = 0.5$ showing the phase-plane attractors associated with inhomogeneous stationary state and phase-locked synchronization states of various phase shifts (Fig4(C,D)).

Discussion

The present modeling study investigates the transition properties between temporally-synchronized and spatially-inhomogeneous patterns driven by the Delta-Notch-Hes signaling axis. To address this issue, we introduced a particular class of discrete cell lattice model where single-cell dynamical repertoire comprises both autonomous oscillatory and switching behaviors. The model could recapitulate a wide spectrum of spatiotemporal behaviors that has been reported over last decades using distinct classes of theoretical models of lateral inhibition. Lateral inhibition itself is a notorious mechanism to generate diverse, and eventually

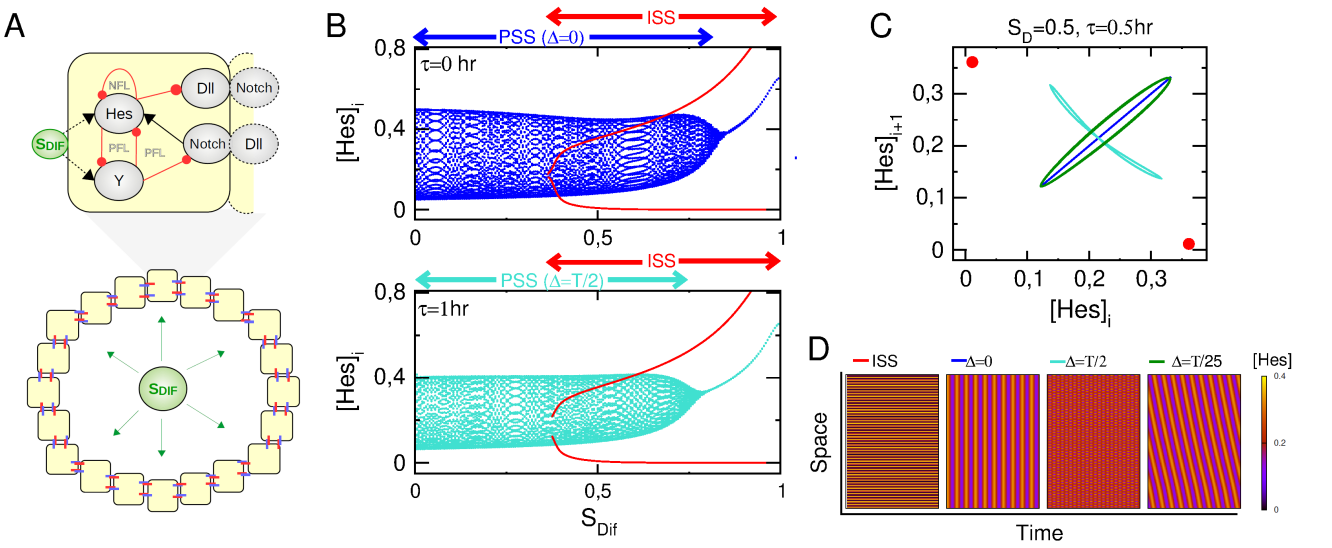

Figure 5: **Multistability between temporally-synchronized and spatially-inhomogeneous states mediated through Delta-Notch-Hes intercellular/intracellular signaling.** (A) One-dimensional ring lattice of Delta-Notch coupled cells. (B) Stability diagram of in-phase (up/blue) or anti-phase (down/turquoise) synchronization state and inhomogeneous stationary state (red) as function of S_{Dif} where $S_{N0,i} = 0.2$, $\Gamma = 1$ and $\tau = 0$ or 1h (i.e., $T/2$). (C) Multistability and coexistence of multiple archetypical (i.e., 2-cell periodic) attractors represented in a relevant section of the state space. Parameters are $S_{N0,i} = 0.2$, $S_{Dif} = 0.5$, $\Gamma = 1$ and $\tau = 0.5$h. (D) Space-time representation of attractors in (C).

multistable, inhomogeneous fine-grained patterns (Collier et al., 1996; Owen et al., 2000; Hadjivasiliou et al., 2016; Hunter et al., 2016), but can also give rise to diverse coherent and synchronization states through time-delayed juxtacrine coupling between oscillatory cells (Lewis, 2003; Morelli et al., 2009; Murray et al., 2011; Wang et al., 2011; Jörg et al., 2015; Tomka et al., 2018). Furthermore, repulsive coupling between synthetic oscillators has been shown to generate a wide range of collective regimes including synchronization states and inhomogeneous stationary states (Ullner et al., 2008; Koseska et al., 2010). By capturing those very diverse collective behaviors as function of a very few parameters (τ, S_D, S_{N0}, Γ), the proposed low-dimensional model proves well-suited to qualitatively study a wide range of developmental processes based on versatile single-cell dynamics, in support or in parallel to more detailed signaling network models.

The extensive multistability reported in the present study builds on several mechanisms and has some implications, notably for pattern selection in different contexts or between functional and spurious ones (Morelli et al., 2009; Palau-Ortin et al., 2015; Pfeuty and Kaneko, 2016; Uriu et al., 2021). Mulistationarity between spatial patterns typically arise from the combination of intrinsic bistability of cells and the intercellular positive feedback through Delta/Notch-mediated lateral inhibition (Collier et al., 1996; Wearing et al., 2000). Multistability between synchronization states is also frequently observed in coupled oscillator systems (Crowley and Epstein, 1989; Morelli et al., 2009; Williams et al., 2013). Less common is the here-characterized multistability between diverse temporally-synchronized and spatially-inhomogeneous states, which entails the existence of many transition paths from a particular temporal pattern to a particular spatial pattern. In addition, signal-driven transition from a stable spatiotemporal pattern toward a given spatial pattern can operate as a both robust and flexible canalization process to the desired multicellular

outcome. This mechanism is complementary to pattern selection and fine-tuning mechanisms mediated by the developmental modulation of Delta-Notch interactions and/or Notch-Delta intracellular signaling (Formosa-Jordan and Ibañes, 2014; Palau-Ortin et al., 2015; Boareto et al., 2015; Sato et al., 2016; Luna-Escalante et al., 2018). This issue of pattern selection is illustrated by the differences observed during neurogenesis and somitogenesis where a similar circuit gives rise either to dynamic salt-and-pepper patterns or traveling waves (Liao and Oates, 2017; Kageyama et al., 2018). It is possible that the desynchronizing action of asymmetric division in the neurogenic case and the synchronizing action of Wnt and Fringe in the somitogenic case could explain diverging spatiotemporal trajectories and outcomes. Another set of differential constraints would relate to the existence of pre-existing boundaries, axis and gradients, for instance related to the layered structure of the developing neural systems or the antero-posterior axis in the somites. In any case, the effective phase-like model could easily incorporate additional constraints at the levels of intercellular coupling or tissue topology to investigate more specific developmental dynamics and reveals how a similar signaling circuitry could give rise to such diversity of developmental patterning processes.

Acknowledgements

This work has been supported by the LABEX CEMPI (ANR-11-LABX-0007) and by the Ministry of Higher Education and Research, Hauts de France council and European Regional Development Fund (ERDF) through the Contrat de Projets Etat-Region (CPER Photonics for Society P4S).

References

Agrawal, S., Archer, C., Schaffer, D.V., 2009. Computational models of the Notch network elucidate mechanisms of context-dependent signaling. PLoS computational biology 5.

Ahnfelt-Rønne, J., Jørgensen, M.C., Klinck, R., Jensen, J.N., Füchtbauer, E.M., Deering, T., MacDonald, R.J., Wright, C.V., Madsen, O.D., Serup, P., 2012. Ptf1a-mediated control of Dll1 reveals an alternative to the lateral inhibition mechanism. Development 139, 33–45.

Andersson, E.R., Sandberg, R., Lendahl, U., 2011. Notch signaling: simplicity in design, versatility in function. Development 138, 3593–3612.

Biga, V., Hawley, J., Soto, X., Johns, E., Han, D., Bennett, H., Adamson, A.D., Kursawe, J., Glendinning, P., Manning, C.S., et al., 2021. A dynamic, spatially periodic, micro-pattern of hes5 underlies neurogenesis in the mouse spinal cord. Molecular systems biology 17, e9902.

Boareto, M., 2020. Patterning via local cell-cell interactions in developing systems. Developmental biology 460, 77–85.

Boareto, M., Jolly, M.K., Lu, M., Onuchic, J.N., Clementi, C., Ben-Jacob, E., 2015. Jagged–delta asymmetry in notch signaling can give rise to a sender/receiver hybrid phenotype. Proceedings of the National Academy of Sciences 112, E402–E409.

Boissonade, J., De Kepper, P., 1980. Transitions from bistability to limit cycle oscillations. Theoretical analysis and experimental evidence in an open chemical system. J. Phys. Chem. 84, 501–506. doi:10.1021/j100442a009.

Collier, J.R., Monk, N.A., Maini, P.K., Lewis, J.H., 1996. Pattern formation by lateral inhibition with feedback: a mathematical model of delta-notch intercellular signalling. Journal of theoretical Biology 183, 429–446.

Crowley, M.F., Epstein, I.R., 1989. Experimental and theoretical studies of a coupled chemical oscillator: phase death, multistability and in-phase and out-of-phase entrainment. The Journal of Physical Chemistry 93, 2496–2502.

Ermentrout, B., 1996. Type i membranes, phase resetting curves, and synchrony. Neural computation 8, 979–1001.

Formosa-Jordan, P., Ibañes, M., 2014. Competition in notch signaling with cis enriches cell fate decisions. PloS one 9, e95744.

Fujimoto, K., Ishihara, S., Kaneko, K., 2008. Network evolution of body plans. PloS one 3, e2772.

Goodfellow, M., Phillips, N.E., Manning, C., Galla, T., Papalopulu, N., 2014. microrna input into a neural ultradian oscillator controls emergence and timing of alternative cell states. Nature communications 5, 3399.

Hadjivasiliou, Z., Hunter, G.L., Baum, B., 2016. A new mechanism for spatial pattern formation via lateral and protrusion-mediated lateral signalling. Journal of the Royal Society Interface 13, 20160484.

Henrique, D., Schweisguth, F., 2019. Mechanisms of Notch signaling: a simple logic deployed in time and space. Development 146, dev172148.

Hunter, G.L., Hadjivasiliou, Z., Bonin, H., He, L., Perrimon, N., Charras, G., Baum, B., 2016. Coordinated control of Notch/Delta signalling and cell cycle progression drives lateral inhibition-mediated tissue patterning. Development 143, 2305–2310.

Jörg, D.J., Morelli, L.G., Soroldoni, D., Oates, A.C., Jülicher, F., 2015. Continuum theory of gene expression waves during vertebrate segmentation. New journal of physics 17, 093042.

Kageyama, R., Ohtsuka, T., Kobayashi, T., 2007. The hes gene family: repressors and oscillators that orchestrate embryogenesis. Development 134, 1243–1251.

Kageyama, R., Shimojo, H., Isomura, A., 2018. Oscillatory control of notch signaling in development. Molecular Mechanisms of Notch Signaling , 265–277.

Keskin, S., Devakanmalai, G.S., Kwon, S.B., Vu, H.T., Hong, Q., Lee, Y.Y., Soltani, M., Singh, A., Ay, A., Özbudak, E.M., 2018. Noise in the vertebrate segmentation clock is boosted by time delays but tamed by notch signaling. Cell reports 23, 2175–2185.

Koseska, A., Ullner, E., Volkov, E., Kurths, J., García-Ojalvo, J., 2010. Cooperative differentiation through clustering in multicellular populations. Journal of theoretical biology 263, 189–202.

Lahmann, I., Bröhl, D., Zyrianova, T., Isomura, A., Czajkowski, M.T., Kapoor, V., Griger, J., Ruffault, P.L., Mademtzoglou, D., Zammit, P.S., et al., 2019. Oscillations of myod and hes1 proteins regulate the maintenance of activated muscle stem cells. Genes & development 33, 524–535.

Laing, C.R., 2016. Travelling waves in arrays of delay-coupled phase oscillators. Chaos: An Interdisciplinary Journal of Nonlinear Science 26, 094802.

Lewis, J., 2003. Autoinhibition with transcriptional delay: a simple mechanism for the zebrafish somitogenesis oscillator. Curr. Biol. 13, 1398–1408.

Liao, B.K., Oates, A.C., 2017. Delta-Notch signalling in segmentation. Arthropod structure & development 46, 429–447.

Luna-Escalante, J.C., Formosa-Jordan, P., Ibañes, M., 2018. Redundancy and cooperation in Notch intercellular signaling. Development 145, dev154807.

Morelli, L.G., Ares, S., Herrgen, L., Schröter, C., Jülicher, F., Oates, A.C., 2009. Delayed coupling theory of vertebrate segmentation. HFSP journal 3, 55–66.

Murray, P.J., Maini, P.K., Baker, R.E., 2011. The clock and wavefront model revisited. Journal of theoretical biology 283, 227–238.

Murray, P.J., Maini, P.K., Baker, R.E., 2013. Modelling delta-Notch perturbations during zebrafish somitogenesis. Developmental biology 373, 407–421.

Nandagopal, N., Santat, L.A., LeBon, L., Sprinzak, D., Bronner, M.E., Elowitz, M.B., 2018. Dynamic ligand discrimination in the Notch signaling pathway. Cell 172, 869–880.

Owen, M.R., 2002. Waves and propagation failure in discrete space models with nonlinear coupling and feedback. Physica D: Nonlinear Phenomena 173, 59–76.

Owen, M.R., Sherratt, J.A., Wearing, H.J., 2000. Lateral induction by juxtacrine signaling is a new mechanism for pattern formation. Developmental biology 217, 54–61.

Palau-Ortin, D., Formosa-Jordan, P., Sancho, J.M., Ibañes, M., 2015. Pattern selection by dynamical biochemical signals. Biophysical journal 108, 1555–1565.

Pfeuty, B., 2015. A computational model for the coordination of neural progenitor self-renewal and differentiation through Hes1 dynamics. Development 142, 477–485. doi:10.1242/dev.112649.

Pfeuty, B., Kaneko, K., 2009. The combination of positive and negative feedback loops confers exquisite flexibility to biochemical switches. Physical Biology 6, 046013.

Pfeuty, B., Kaneko, K., 2014. Reliable binary cell-fate decisions based on oscillations. Phys. Rev. E 89, 022707. doi:10.1103/PhysRevE.89.022707.

Pfeuty, B., Kaneko, K., 2016. Requirements for efficient cell-type proportioning: regulatory timescales, stochasticity and lateral inhibition. Physical Biology 13, 026007.

Plahte, E., Øyehaug, L., 2007. Pattern-generating travelling waves in a discrete multicellular system with lateral inhibition. Physica D: Nonlinear Phenomena 226, 117–128.

Roese-Koerner, B., Stappert, L., Berger, T., Braun, N.C., Veltel, M., Jungverdorben, J., Evert, B.O., Peitz, M., Borghese, L., Brüstle, O., 2016. Reciprocal regulation between bifunctional miR-9 and its transcriptional modulator notch in human neural stem cell self-renewal and differentiation. Stem cell reports 7, 207–219.

Sagner, A., Gaber, Z.B., Delile, J., Kong, J.H., Rousso, D.L., Pearson, C.A., Weicksel, S.E., Melchionda, M., Gharavy, S.N.M., Briscoe, J., et al., 2018. Olig2 and Hes regulatory dynamics during motor neuron differentiation revealed by single cell transcriptomics. PLoS biology 16, e2003127.

Sato, M., Yasugi, T., Minami, Y., Miura, T., Nagayama, M., 2016. Notch-mediated lateral inhibition regulates proneural wave propagation when combined with egf-mediated reaction diffusion. Proceedings of the National Academy of Sciences 113, E5153–E5162.

Shaya, O., Binshtok, U., Hersch, M., Rivkin, D., Weinreb, S., Amir-Zilberstein, L., Khamaisi, B., Oppenheim, O., Desai, R.A., Goodyear, R.J., et al., 2017. Cell-cell contact area affects notch signaling and notch-dependent patterning. Developmental cell 40, 505–511.

Siebel, C., Lendahl, U., 2017. Notch signaling in development, tissue homeostasis, and disease. Physiological reviews 97, 1235–1294.

Sjöqvist, M., Andersson, E.R., 2019. Do as i say, not (ch) as i do: Lateral control of cell fate. Developmental biology 447, 58–70.

Sprinzak, D., Lakhanpal, A., LeBon, L., Santat, L.A., Fontes, M.E., Anderson, G.A., Garcia-Ojalvo, J., Elowitz, M.B., 2010. Cis-interactions between Notch and Delta generate mutually exclusive signalling states. Nature 465, 86–90.

Stanoev, A., Schröter, C., Koseska, A., 2021. Robustness and timing of cellular differentiation through population-based symmetry breaking. Development 148, dev197608.

Suzuki, N., Furusawa, C., Kaneko, K., 2011. Oscillatory protein expression dynamics endows stem cells with robust differentiation potential. PloS one 6, e27232.

Tiedemann, H.B., Schneltzer, E., Beckers, J., Przemeck, G.K., de Angelis, M.H., 2017. Modeling coexistence of oscillation and Delta/Notch-mediated lateral inhibition in pancreas development and neurogenesis. Journal of theoretical biology 430, 32–44.

Tomka, T., Iber, D., Boareto, M., 2018. Travelling waves in somitogenesis: collective cellular properties emerge from time-delayed juxtacrine oscillation coupling. Progress in biophysics and molecular biology 137, 76–87.

Ullner, E., Koseska, A., Kurths, J., Volkov, E., Kantz, H., García-Ojalvo, J., 2008. Multistability of synthetic genetic networks with repressive cell-to-cell communication. Physical Review E 78, 031904.

Uriu, K., Liao, B.K., Oates, A.C., Morelli, L.G., 2021. From local resynchronization to global pattern recovery in the zebrafish segmentation clock. Elife 10, e61358.

Vasconcelos, F.F., Sessa, A., Laranjeira, C., Raposo, A.A., Teixeira, V., Hagey, D.W., Tomaz, D.M., Muhr, J., Broccoli, V., Castro, D.S., 2016. Myt1 counteracts the neural progenitor program to promote vertebrate neurogenesis. Cell reports 17, 469–483.

Wahi, K., Bochter, M.S., Cole, S.E., 2016. The many roles of notch signaling during vertebrate somitogenesis, in: Seminars in cell & developmental biology, Elsevier. pp. 68–75.

Wang, R., Liu, K., Chen, L., Aihara, K., 2011. Neural fate decisions mediated by trans-activation and cis-inhibition in notch signaling. Bioinformatics 27, 3158–3165.

Wearing, H., Owen, M., Sherratt, J., 2000. Mathematical modelling of juxtacrine patterning. Bulletin of mathematical biology 62, 293–320.

Williams, C.R., Sorrentino, F., Murphy, T.E., Roy, R., 2013. Synchronization states and multistability in a ring of periodic oscillators: Experimentally variable coupling delays. Chaos: An Interdisciplinary Journal of Nonlinear Science 23, 043117.